AIAA 2002-0124
Sensitivity of Synthetic Jets to the Design of the Jet Cavity

Y. Utturkar
Department of Mechanical Engineering,
University of Florida, Gainesville, FL-32611

R. Mittal
Department of Mechanical and Aerospace Engineering
The George Washington University, Washington DC 20052

P. Rampunggoon
Department of Mechanical Engineering,
University of Florida, Gainesville, FL-32611

L. Cattafesta
Department of Aerospace Engineering, Mechanics and Engineering Science
University of Florida, Gainesville, FL-32611

40th AIAA Aerospace Sciences Meeting & Exhibit
14-17 January 2002 / Reno, NV

Sensitivity of Synthetic Jets to the Design of the Jet Cavity

Y. Utturkar[1], R. Mittal[2], P. Rampunggoon[1] and L. Cattafesta[3]

[1]Department of Mechanical Engineering
University of Florida
Gainesville, Florida, 32611

[2]Department of Mechanical and Aerospace Engineering
The George Washington University
Washington DC 20052

[3]Department of Aerospace Engineering, Mechanics and Engineering Sciences
University of Florida
Gainesville, FL 32611

ABSTRACT

The sensitivity of synthetic jets to the design of the jet cavity is examined using numerical simulations. In this study, the primary focus is on examining the effect of changes in the cavity aspect ratio and the placement of piezoelectric diaphragm on the flow produced by the jet. Cases with and without an external cross-flow are investigated. This study compares the vortex dynamics, velocity profiles and other dynamical characteristics of the jet for the various cases and this allows us to extract some insight into the effect of these modifications on the jet performance. It is expected that this study will prove useful in the design as well as in developing dynamical models for these devices.

1. INTRODUCTION

The synthetic jet has emerged as one of the most useful mico (or meso) fluidic devices with the potential application ranging from thrust vectoring jet engines (Smith et al. 1997), mixing enhancement (Chen et al. 1999, Davis et al 1999) to active control of separation and turbulence in boundary layers (Amitay et al. 1997, Smith & Glezer 1998, Crook et al 1999). A detailed parametric study of the synthetic jet (Mittal et al. 2001, Rampunggoon 2001) has been carried out using numerical simulations where the effect of variation in jet operational parameters (diaphragm amplitude and slot dimensions) as well as external flow characteristics has been examined. However in the practical applications, design constraints could necessitate modifications in the shape of the design cavity as well as in the placement of the piezoelectric diaphragm. Thus it is useful to examine the effect that the variation of these factors has on the jet and this forms the motivation for the current study.

2. FLOW CONFIGURATION AND SIMULATION APPROACH

Flow Configuration

Consider the synthetic jet device in Figure 1, which is attached beneath a flat plate on which develops a laminar Blasius boundary layer. The synthetic jet is created at the slot by the oscillation of a diaphragm attached to the bottom of the jet cavity and the diaphragm deflection is characterized by the deflection amplitude (A) and angular frequency (ω). The cavity, which is rectangular in shape, is defined by the cavity width (W) and the cavity height (H). A slot type exit is chosen for the jet and this orifice is characterized by a height (h) and width (d). The exterior flow, which consists of a laminar Blasius boundary layer, is characterized by a freestream velocity (U_∞) and boundary layer thickness (δ). Finally, the fluid is characterized by its kinematic viscosity (ν) and density (ρ).

Additional parameters need to be considered in the situation where compressibility effects inside the cavity become significant. Indeed, changes in the cavity shape and the placement of the diaphragm might alter the acoustic characteristics of the cavity. Therefore inclusion of compressibility effects might be of great interest in such an investigation. However, in the current study we focus on incompressible flow simulations only.

Jet Characterization and Scaling

The flow emerging from the slot is in principle a function of all the parameters described in the paragraph above. The exit flow, which is both a function of space and time, can be characterized via a number of different parameters. In our previous studies, we have advocated employing successive moments of the jet velocity profile as a more general approach to charactering the jet behavior. The n^{th} moment of the jet $C^n_{\phi_{12}}$ is defined as

$$C^n_{\phi_{12}} = \frac{1}{\phi_2 - \phi_1}\frac{1}{d}\int_{\phi_1}^{\phi_2}\int_{-d/2}^{d/2}\left[V_J(x,\phi)\right]^n dx\, d\phi \qquad (1)$$

where V_J is the jet velocity normalized by suitable velocity scale (freestream velocity or maximum inviscid jet velocity). Our preliminary simulations indicate that the jet flow is significantly different in the ingestion and expulsion phases and characterizing this difference is the key to understanding the physics of this flow. Thus it is natural to define the moment separately for the ingestion and expulsion phases and these are denoted by C^n_{in} and C^n_{ex} respectively. This hierarchical characterization provides a systematic framework for the development of scaling laws. Furthermore, a number of these moments have direct physical significance. For instance $C^1_{in} + C^1_{ex}$ corresponds to the jet mass flux (which is identically equal to zero for a synthetic jet) whereas $C^2_{in} + C^2_{ex}$ and $C_{in}{}^3 + C_{ex}{}^3$ correspond to the momentum and kinetic energy flux of the jet. Using the Buckingham Pi theorem, the functional dependence of these parameters can be written in terms of non-dimensional parameters as:

$$\left(C^n_{in}; C^n_{ex}\right) = fn\left(\frac{W}{H}, \frac{A}{H}, \frac{d}{h}, \frac{d}{W}, \sqrt{\frac{\omega d^2}{\nu}}, \frac{U_\infty \delta}{\nu}, \frac{\delta}{d}\right) \qquad (2)$$

where

W/H:	cavity width to height ratio of cavity
A/H:	stroke length to cavity height ratio
h/d:	aspect ratio of slot
d/W:	slot to cavity width ratio
$\sqrt{\omega d^2/\nu} = S$:	Stokes number
$U_\infty \delta/\nu = \mathrm{Re}_\delta$:	boundary layer thickness Reynolds number
δ/d :	ratio of boundary layer thickness to slot width

In past studies we have investigated the effect of varying *A/H* , *h/d,* Re_δ and δ/d (R. Mittal et al. 2001, P. Rampunggoon 2001) on the jet. In the current study, the focus is on examining the variation in the diaphragm placement and cavity aspect ratio *W/H*. One parameter found useful in the normalization of the jet velocity is the maximum inviscid velocity $V^{\max}_{inv}$ which is given by $Q_{\max}/d$ where $Q_{\max}$ is the maximum volume flux per unit spanwise depth of the jet.

Simulation Approach

A previously developed Cartesian grid solver (Udaykumar et al. 1999, Ye et al. 1999, Udaykumar et al 2001) is being employed in these simulations. Details of the solution procedure can be found in these papers. This solver allows simulation of unsteady viscous incompressible flows with complex immersed moving boundaries on Cartesian grids. Thus, the grid does not need to conform to the complex moving boundaries and this simplifies the gridding of the flow domain. This solver employs a second-order accurate central difference scheme for the spatial discretization and a mixed explicit-implicit fractional step scheme for time advancement. An efficient multigrid algorithm is used for solving the pressure Poisson equation.

The key advantage of this solver for the current flow is that the entire geometry of the synthetic jet including the oscillating diaphragm is modeled on the stationary Cartesian mesh. Figure 2 shows the typical mesh used in the simulations. As the diaphragm moves over the underlying Cartesian mesh, the discretization in the cells cut by the solid boundary is modified to account for the presence of the solid boundary. In addition, suitable boundary conditions also need to be prescribed for the external flow. For the quiescent external flow case, a soft velocity boundary condition is applied on the north, east and west boundaries that allow the conditions at these boundaries to respond freely to the flow created by the jet. For the simulation of jet in a cross-flow, inflow boundary conditions corresponding to a Blasius boundary layer profile are imposed at the west boundary whereas soft boundary conditions are applied at the north and east boundaries. All simulations are run until initial transients decay and statistics are accumulated beyond this over a number of cycles.

3. SIMULATION RESULTS

In this section, we describe the vortex dynamics observed for some selected cases. Four different designs of the jet cavity are investigated and for each of these, simulation are carried out with and without and external cross flow. In the cases with external flow, the boundary layer Reynolds number is fixed at Re_δ=1200. The modifications in the cavity design are subjected to two constraints viz. the cavity volume and the cumulative volume displacement of the diaphragms are constant.

Cavity Designs

Figure 3 shows a schematic of the five different cavity designs examined in the current study. Case 1 consists of a cavity with aspect ratio *W/H*=5 and the piezoelectric diaphragm is fixed to the lower wall of the cavity. This particular case has been studied extensively in the past (Mittal et al. 2001, Rampunggoon 2001). Case 2 consists of a cavity with aspect ratio *W/H*=1/5 and the diaphragm is fixed to the right wall of the cavity. Case 3 has a cavity with the same shape as Case 2 except, in this case, diaphragms are fixed to *both* side-walls. The amplitude of vibration of these diaphragms is one-half that of the previous two cases in order to maintain the same expulsion flux. Case 4 and 5 consist of square cavities where, for Case 4, the diaphragm is located only on the lower wall. In

Case 5, both side walls as well as the bottom wall have oscillating diaphragms. All other parameters are kept fixed in the current simulation. In particular S=10.0 and h/d=1 and, for the external crossflow cases, Re_δ is fixed at 1200. In the following we first compare the performance of the jets with quiescent external flow. This is followed up by a similar comparison in the situation where there is an external crossflow.

Jet in Quiescent External Flow

Figure 4 shows contours plots of spanwise vorticity for all the cases after the flow has reached a stationary state and this provides a qualitative view of the effect of the modification of the structure on the vortices produced by the jet. It is observed that despite the significant differences in the cavity design all cases except for Case 2 produce virtually the same external flow. Thus, the large differences in the internal cavity flow do not translate into similar differences in the external flow. Among all the cases simulated here, Case 2 is the only one with a diaphragm arrangement that is asymmetrical about the vertical centerline of the cavity. This arrangement produces a highly asymmetric flow in the cavity, which in turn produces a vortex dipole outside the slot during expulsion that is also slightly asymmetric. This asymmetry produces a self-induced velocity on the dipole that has a small horizontal component thereby resulting in a noticeable horizontal drift in the dipoles as they are propelled upwards. As has been noted before (Rampunggoon 2001) the extent to which asymmetries in the cavity flow can effect the external flow depends primarily on the slot aspect ratio h/d. It has been found that at least in the range of parameters investigated here, asymmetries produced in the jet cavity tend to dampen as the flow passes through the slot. Therefore, higher values of h/d (which imply a longer slot) typically produce more symmetric external jet flows. The horizontal drift in the vortex dipole might have some important implications in impingement heat transfer type applications of synthetic jets (Campbell et al. 1998, Guarino et al. 2001) where precise "targeting" of high temperature sites by the dipoles would be desirable.

Further insight into the effect of the cavity modifications on the jet can be gained by examining the jet velocity profile at the slot exit. Figure 5 shows these profiles for the various cases at four different phases in the cycle. Overall no significant difference in the velocity profile is observed. However, both Cases 2 and 3 both of which have cavities with $H > W$, the peak velocity at maximum expulsion is somewhat higher than the other cases. Furthermore, the inherent asymmetry in Case 2 is apparent in the jet velocity profile which clearly shows that for this case, the jet velocity profile is slightly asymmetric about the slot center line. This slight asymmetry creates a vortex dipole that has a slightly stronger clockwise vortex and this results in the rightwards horizontal drift in the vortex dipole.

The performance of the jet is often characterized in terms of the jet momentum coefficient C^2. In our previous work (R. Mittal et al. 2001, P. Rampunggoon 2001) we have found it useful to normalize momentum coefficient by the coefficient corresponding to an inviscid jet (with a uniform jet profile) at the same operating condition of the jet. In Table 1 we present the normalized jet momentum coefficient for all the cases simulated here. Coefficients have been calculated separately for the expulsion and ingestion phases in the cycle and a total for the entire cycle is also presented. The separation into the ingestion and expulsion strokes allows us to examine in detail, the effect of the cavity modification on the jet performance.

The table indicates an average value of total momentum coefficient for all the cases of 1.2 implying that the momentum flux of the jet is 20% higher than that of an inviscid jet. The root-mean square variation about this average value is equal to about 0.03 which amount to a 2.5% variation. Therefore, the current set of simulations of the synthetic jet in a quiescent external flow indicates that the overall effect of the cavity design changes on the jet momentum coefficient is quite small. During the expulsion phase, flow from inside the cavity is expelled out through the slot and therefore it is expected that modification in the cavity design will have a larger effect on the expulsion flow. This is borne out in the current simulations since we find that the standard deviation in the momentum coefficient during ingestion is 1.4% of its mean value whereas that in the expulsion is 3.7%. It should be noted that the momentum coefficient is an integral measure of the jet profile at the jet exit and does not provide any direct indication of the behavior of the jet as it convects away from the slot. Thus, even though for Case 2, the jet exhibits a significant horizontal drift, this difference in behavior is not necessarily reflected in the momentum coefficient.

Jet in External Cross-Flow

In this section we describe the simulations results for the same five cases discussed in the previous section, except that here, an external cross-flow is imposed on the jet. The external flow corresponds to a Blasius flat-plate boundary layer with a boundary layer thickness based Reynolds number $\mathrm{Re}_\delta = 1200$. Figure 6 shows spanwise vorticity plots for the five cases at a phase in the cycle where the diaphragm has maximum upwards deflection. The flow inside the cavity is highly asymmetric for all cases due to the imposed external cross flow. All cases show the formation of a shear layer at the jet exit with clearly discernible sequence of clockwise rotating vortices. Thus, the vortex-dipole structure visible for the cases with quiescent external flow is replaced here by an unstable shear layer. Although there are some qualitative differences in the vortex structures, it is fair to state that these differences are not significant and also do not reveal any obvious trends. The computed velocity profiles at the jet exit (Figure 7) also show some differences between the various cases, especially during the expulsion stage. Table 2 shows the computed normalized momentum coefficients and for all the cases simulated here, the average total normalized momentum coefficient is 1.36 with a standard deviation of about 7% of its mean value. Thus clearly, the jet is more sensitive to modifications in the cavity design in the presence of the external cross-flow. However, wide ranging

modifications in the cavity design still yield only modest changes in the synthetic jet.

4. CONCLUSIONS

Numerical simulations have been used to study the sensitivity of synthetic jets to the design of the jet cavity. Design changes examined include changes in the cavity aspect ratio as well as placement of the oscillating diaphragms. Synthetic jets in quiescent as well as external cross-flow have been investigated. The general conclusion is that wide-ranging modifications in the cavity design have a relatively limited effect on the jet exit flow. Integral parameters of the jet exit velocity profile such as the momentum coefficient show less than a 7% deviation for all the different cases examined in the current study. One case where significant differences are observed in the evolution of the jet is the design with asymmetric placement of the diaphragm in quiescent external flow. For this case, the asymmetric cavity flow creates a asymmetric vortex dipole in the external flow and this dipole is observed to undergo a significant horizontal drift. This might be of some importance in impingement heat transfer applications of synthetic jets where targeting of localized "hot" sites by the jet is required.

The current results have significant implications for the design, deployment and modeling of these devices since they indicate that the details of the cavity design and diaphragm placement do not play a crucial role in determining the performance of the jet. Therefore these factors may be modified as required to satisfy design/deployment constraints without much concern for any adverse effects on the jet performance. From the point of view of computational/theoretical modeling of these devices also, the current study indicates that if the interest is primarily in modeling/predicting the external jet flow, rough models of the cavity might suffice. The caveats are that firstly, the range of parameters studied here is limited both in scope as well as range and therefore it is difficult to draw universal conclusions from this study. Second, the current study does not take account of compressibility effects and it is expected that a compressible flow inside the cavity will be more sensitive to the cavity design. This remains to be examined through either numerical simulations or experiments.

ACKNOWLEDGEMENT

This work is supported by NASA grant NAG-1-01024 monitored by Susan Gorton. Computer time for these simulations has been provided by a startup grant from NCSA at the University of Illinois at Urbana-Champaign.

REFERENCES

Amitay, M., Honohan, A., Trautman, M., Glezer, 1997. A. Modification of the Aerodynamic Characteristic of Bluff Bodies Using Fluidic Actuators. AIAA 97-2004.

Amitay, M., Smith, B. L., Glezer, A.1998. Aerodynamic Flow Control Using Synthetic Jet Technology. AIAA 98-0208.

Campbell, J., Black, W. Z., Glezer, A., 1998. Thermal Management of a Laptop Computer with Synthetic Air Microjets, Thermal and Thermomechanical Phenomena in Electronic Systems, Page 43-50

Chen, Y., Liang, S., Aung, K., Glezer, A., Jagoda, J. 1999. Enhanced Mixing in a Simulated Combustor Using Synthetic Jet Actuators. AIAA 99-0449.

Crook, A., Sadri, A. M., Wood, N. J. 1999. The Development and Implementation of Synthetic Jets for the Control of Separated Flow. AIAA 99-3176.

Davis, S. A., Glezer, A. 1999. Mixing Control of Fuel Jets Using Synthetic Jet Technology : Velocity Field Measurement. AIAA 99-0447.

Guarino, J., Manno, V., 2001. Characterization of Laminar Jet Impingement Cooling in Portable Computer Applications. Seventeenth Annual IEEE Symposium , Page 1-11

Mittal, R., Rampuggoon, P., Udaykumar, H. S. 2001. Interaction of a Synthetic Jet with a flat plate boundary layer. AIAA 2001-2773.

Rampunggoon, P. 2001 Interaction of a Synthetic Jet with a Flat-Plate Boundary Layer. Ph.D. Thesis, Dept. of Mech. Engr., University of Florida, Gainesville, FL 32611.

Smith, B.L., Glezer A. 1997. Vectoring and Small-scale Motions Effected in free Shear Flows Using Synthetic Jet Actuators. AIAA 97-0213

Smith, D., Amitay, M., Kibens, V., Parekh, D., Glezer, A. 1998b. Modification of Lifting Body Aerodynamics Using Synthetic Jet Actuators. AIAA 98-0209.

Smith, D. R., Kibens, V., Pitt, D. M., Hopkins, M. A. 1999b. Effect of Synthetic Jet Arrays on Boundary Layer Control. SPIE. Vol. 3674.

Udaykumar, H. S., Mittal R., and Shyy, W. Solid-Liquid Phase Front Computations in the Sharp Interface Limit on Fixed Grids. *J. Comp. Phys*. Vol. 18, pp. 535-574 (1999).

Udaykumar, H.S., Mittal, R., Rampunggoon, P. and Khanna, A. A Sharp Interface Cartesian Grid Method for Simulating Flow with Complex Moving Boundaries. To appear in *J. Comp. Phys.* Vol. 174, 2001.

Ye, T., Mittal, R., Udaykumar, H. S., Shyy, W., 1999. An accurate Cartesian grid method for viscous incompressible flows with complex immersed boundaries, *J. Comp. Phys*., Vol. 156, pp. 209-240.

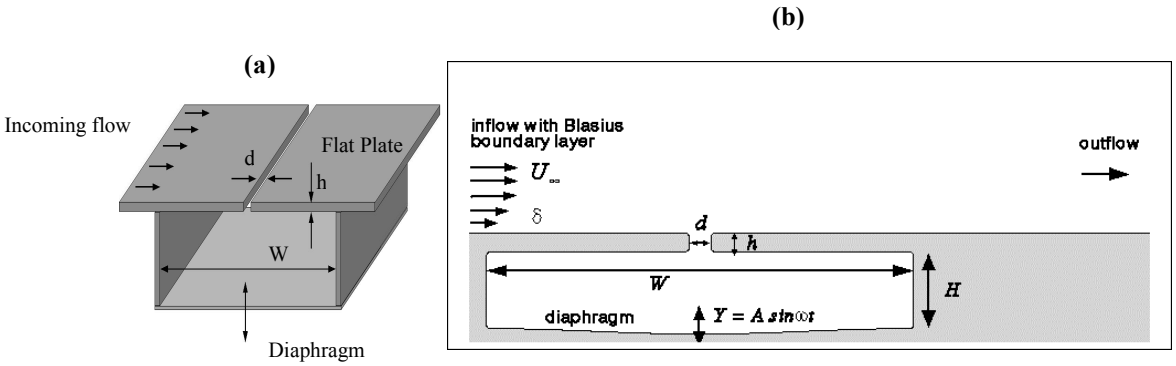

Figure 1. (a) Schematic diagram of a synthetic jet actuator with the rectangular chamber and slot
(b) The configuration of a 2-D synthetic jet used in the study

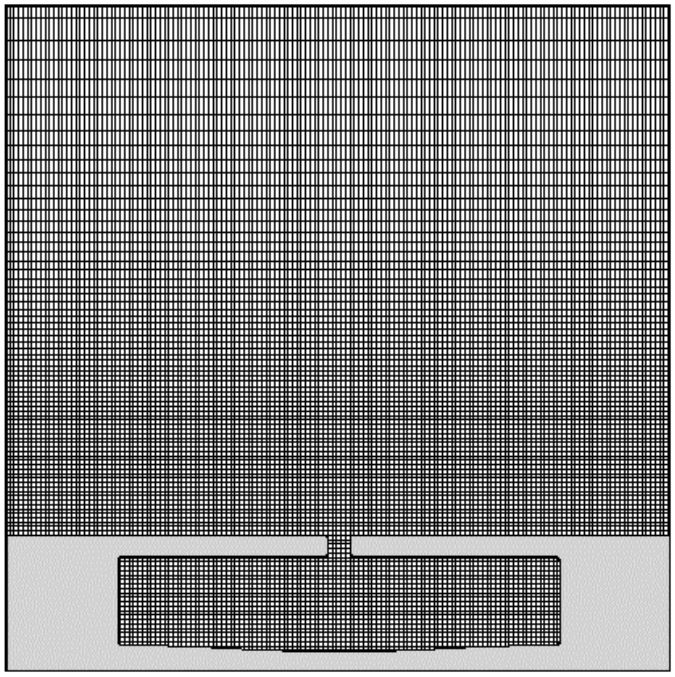

Figure 2. A fixed non-uniform Cartesian grid used in the
synthetic jet calculation. Every third grid point is shown

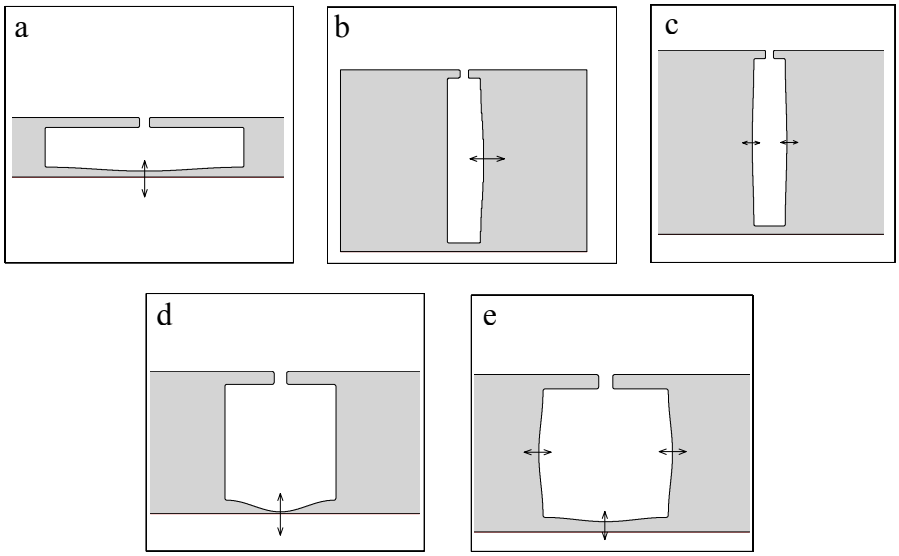

Figure 3. Shape of the jet cavities used in the study (a) Case 1 (b) Case 2 (c) Case 3 (d) Case 4 (e) Case 5

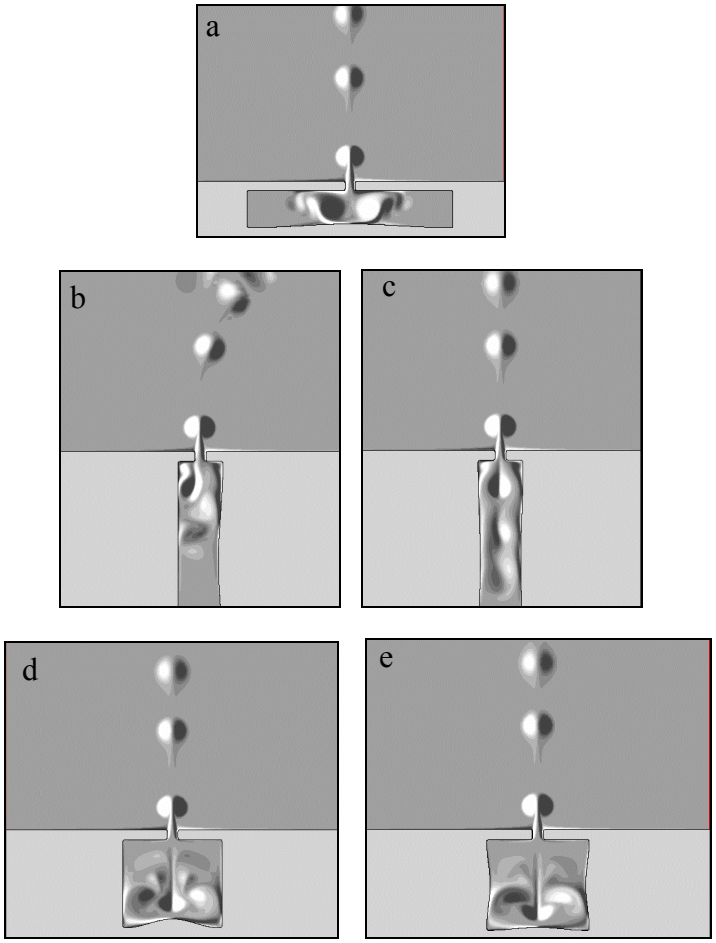

Figure 4. Plot of vorticity contour for the five cases extracted at the minimum volume phase of the expulsion stroke, $Re_\delta=0$ (a) Case 1 (b) Case 2 (c) Case 3 (d) Case 4 (e) Case 5

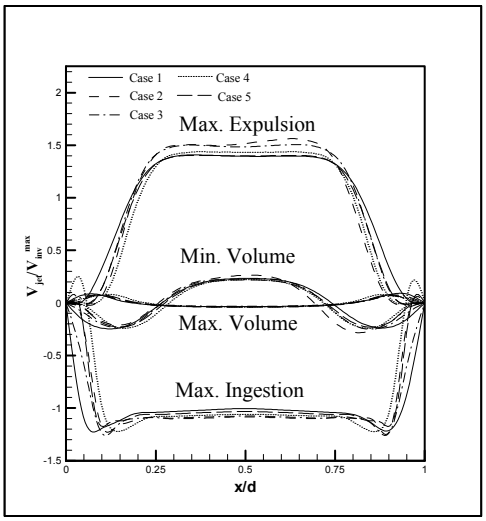

Figure 5. Velocity profiles at the exit of the Jet Orifice (Re_δ=0)

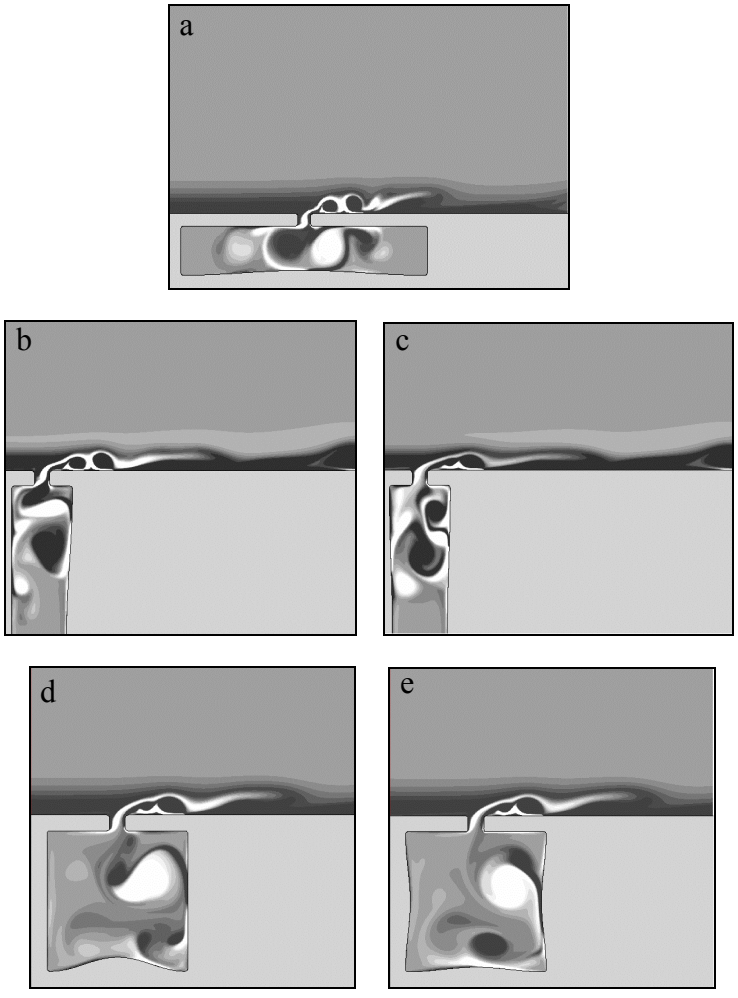

Figure 6. Plot of vorticity contour for the five cases extracted at the minimum volume phase of the expulsion stroke, Re_δ=1200
(a) Case 1 (b) Case 2 (c) Case 3 (d) Case 4 (e) Case 5

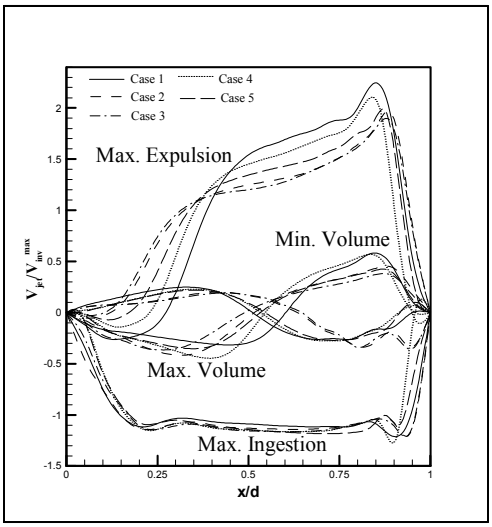

Figure 7. Velocity profiles at the exit of the Jet Orifice (Re_δ=1200)

Case	C^2_{in}	C^2_{ex}	C^2_{Tot}
Case 1	1.07	1.26	1.17
Case 2	1.09	1.39	1.24
Case3	1.09	1.36	1.23
Case 4	1.10	1.31	1.21
Case 5	1.06	1.28	1.17
Average	1.08	1.32	1.20
Std. Dev.	0.015	0.049	0.029

Table 1. Normalized momentum coefficients for quiescent flow

Case	C^2_{in}	C^2_{ex}	C^2_{Tot}
Case 1	1.13	1.91	1.52
Case 2	1.14	1.45	1.30
Case3	1.15	1.40	1.27
Case 4	1.15	1.67	1.41
Case 5	1.11	1.49	1.30
Average	1.13	1.58	1.36
Std. Dev.	0.015	0.187	0.093

Table 2. Normalized momentum coefficients for external flow